Electronic Supplementary Information (ESI)

Surface topology of MXene flakes induces the selection of the sintering mechanism for supported Pt nanoparticles

Jiawei Huang,[a] Yucheng Zhang,[a] Jiaqi Chen,[a] Zhouyang Zhang,[b] Chunfang Zhang,[c] Changshui Huang*[d] and Linfeng Fei*[a]*

[a] School of Physics and Materials Science, Nanchang University, Nanchang 330031, China.

[b] School of Materials and New Energy, Ningxia University, Yinchuan 750021, China

[c] College of Chemistry and Materials Science, Hebei University, Baoding 071002, China.

[d] Beijing National Laboratory for Molecular Sciences, Organic Solids Laboratory, Institute of Chemistry, Chinese Academy of Sciences, Beijing 100190, China.

E-mail: feilinfeng@gmail.com (L.F.); zhangcf@hbu.edu.cn (C.Z.); huangcs@iccas.ac.cn (C.H.)

Contents of Supplementary Information:

1. Methods

1-1. Preparation of TEM specimen

MXene flakes: We used commercial MXene sample as the starting material (after MAX etching, purchased from Jilin 11 Technology Co., Ltd.). To gain monolayer $Ti_3C_2T_x$ MXene flakes, 10 ml of MXene solution was dispersed in 20 ml of deionized water, which was then sonicated under Ar gas for 2 hours. The exfoliated MXene flakes were dispersed in ethanol solution to form a precursor solution, which was sonicated for another 20 min before use.

Pt nanoparticle precursor: $(NH_3)_4Pt(NO_3)_2$ was dissolved in ethanol to form a Pt precursor solution, and was sonicated for 20 min before use.

Pt/MXene nanocatalyst: Firstly, the MXene precursor solution was dropped on a heating E-chip specimen support and naturally dried in air. Afterwards, we used a Gatan Solarus II plasma cleaner to treat MXene surface with Ar^+/O^{2-} bombardment at a flow rate of 30 sccm for 60 s. The vacuum pump valve was set to 350 mTorr, and the power parameter was set to 40 W. Finally, the Pt/MXene sample was prepared by drop-casting the Pt precursor solution on the heating E-chip with MXene flakes.

1-2. Aberration-corrected STEM characterization

The atomic-scale morphology of MXene and Pt/MXene as well as EDS elemental mappings were captured on a 300 kV double-aberration-corrected Titan Themis Z electron microscope.

1-3. In situ (S)TEM experiment

In situ (S)TEM experiment in this work was performed with a DENSsolutions Wildfire heating holder. TEM experiment was conducted on a JEOL JEM-F200 cold-field-emission TEM operated at 200 kV, equipped with a dual silicon drift detectors (SDDs) EDS and a Gatan Continuum S EELS. TEM images were recorded using a Gatan OneView IS camera with an optimized exposure time. STEM images were recorded using a Gatan PEELS camera with ~30 s exposure time. For TEM heating experiments, the sample was heated from RT to 800 ^oC in 50 ^oC increments with a ramping rate of

5 ^{o}C s^{-1}. After each 50 ^{o}C increment, the sample temperature was held for 30 min for (S)TEM imaging. Noteworthy, the beam valve was closed during each heating step to minimize the electron beam effects. The in situ experiments were implemented repeatedly to confirm the structural evolution dynamics as reported. To monitor the influence of electron beam irradiation on the sintering dynamics, we compared the observed area with the places not exposed to continuous e-beam after every heating step.

1-4. Computational details

DFT calculations were performed by using the Vienna ab initio simulation package (VASP). The exchange-correlation interaction was described by the generalized gradient approximation (GGA) with the Perdew-Burke-Ernzerhof (PBE) scheme.[1] For all calculations, Grimme's DFT-DF method was used to include the van der Waals correction and the energy cut-off was set to 550 eV.[2] The convergence thresholds of the total energy was set to be 10^{-6}.

The primitive cell with 6 Ti and 4 C was constructed and optimized firstly with the Brillouin zone was sampled by Monkhorst-Pack k-point grid of 7 × 7 × 7 mesh, and then expanded to the 8 × 8 × 2 supercell with the Monkhorst-Pack k-point grid mesh of 1 × 1 × 1 to investigate the metal support interaction. The two layer slabs of the 8×8×2 supercell containing 384 Ti and 256 C atoms with a 15 Å vacuum were constructed and optimized to simulate the non-interacting surface. Furthermore, two surfaces with defects in the first layer were constructed, where 136 Ti and 116 C atoms were eliminated from the 8 × 8 × 2 supercell (def-sc882) and the Pt_5 cluster adsorbed at different positions were also constructed to explore the topology effect of MXene flakes.

The absorption energy (E_{abs}) for the Pt_5 cluster at different positions of the surfaces was calculated by Equation (1):

E_{abs}=E_total-E_(support)-E_(Pt_5) (1)

In which E_total is the total energy for the Pt_5 cluster adsorbed on the def-sc882 surface, E_(support) is the energy of the def-sc882 surface, and E_(Pt_5) refers to the

energy of the Pt_5 cluster.

2. Supporting figures

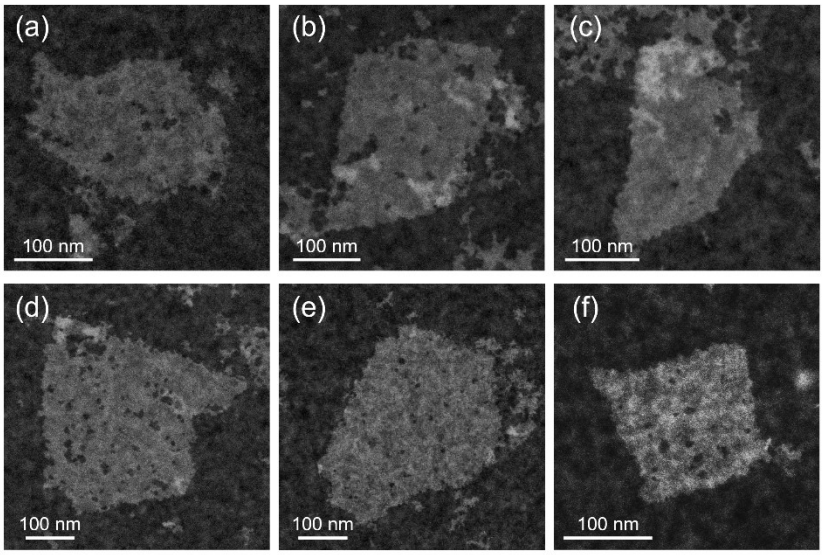

Figure S1. (a-c) STEM images of the pristine MXene surface. (d-f) STEM images of the cleaved MXene surface after the treatment of Ar^{+}/O^{2-} bombardment, showing no noticeable change compared to the pristine MXene surfaces.

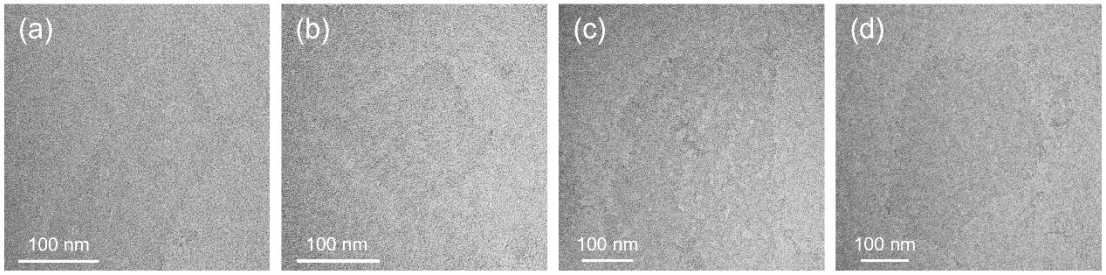

Figure S2. (a-d) Bright-field TEM images showing the typical morphologies for MXene flakes.

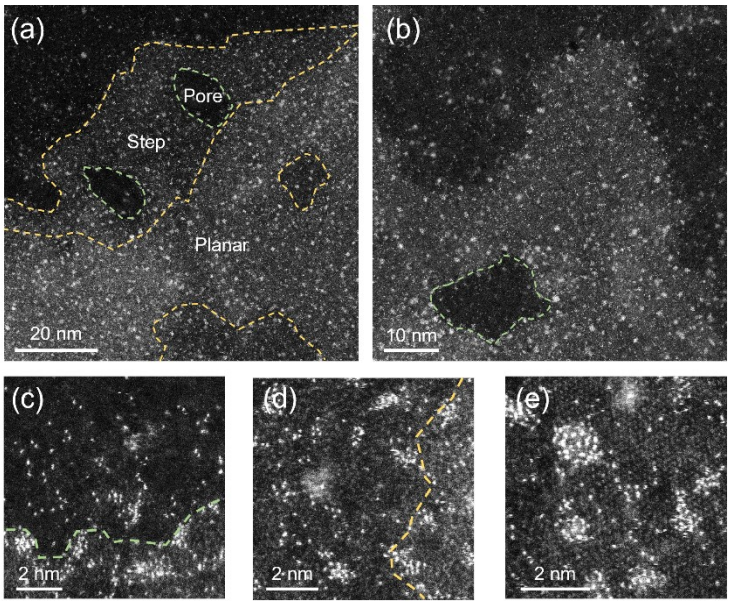

Figure S3. (a, b) Low-magnification STEM images showing Pt atoms or NPs on the different regions of MXene flakes. (c-e) Magnified STEM images showing the existence of Pt atoms or NPs on pores, steps and planar surfaces of MXene flakes, respectively.

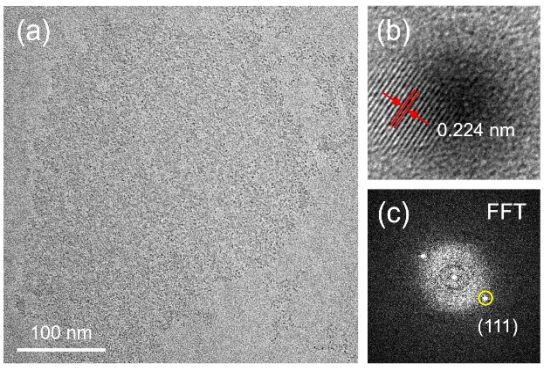

Figure S4. (a) TEM image of the Pt/MXene nanocatalyst after heating to 800 ^{o}C. (b) HRTEM image of the supported Pt NPs on the MXene surface. (c) The corresponding fast Fourier transform (FFT) patterns for (b).

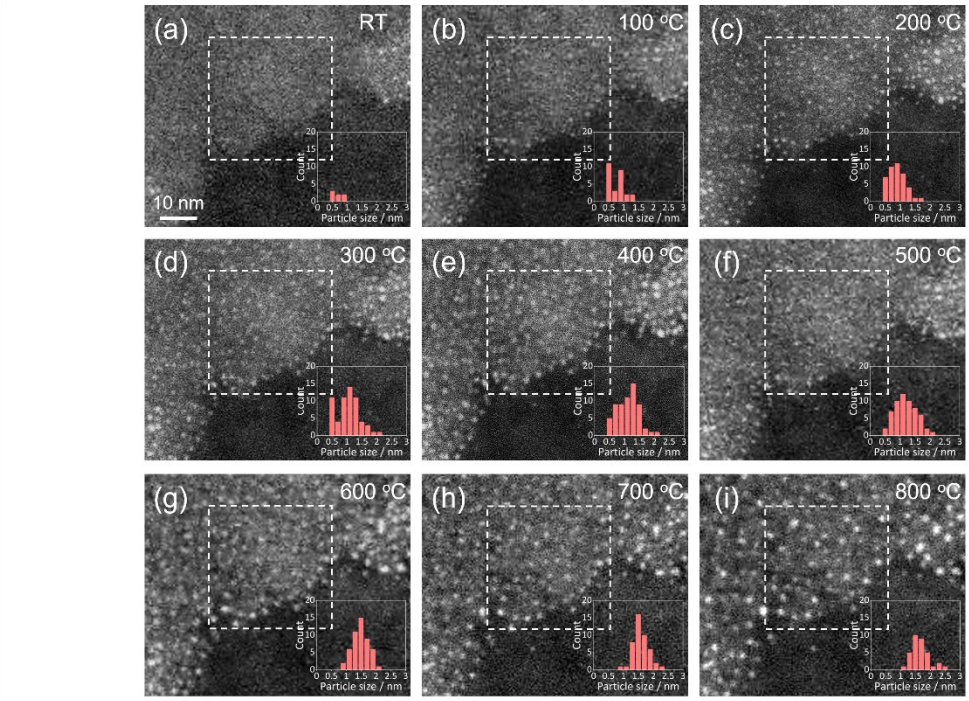

Figure S5. (a-i) In situ STEM images of Pt NPs on MXene flakes against the rising temperature. The inset in each frame of (a-i) corresponds to the size distribution of Pt NPs in the dashed boxes. The scale bar in (a) also applies to (b-i).

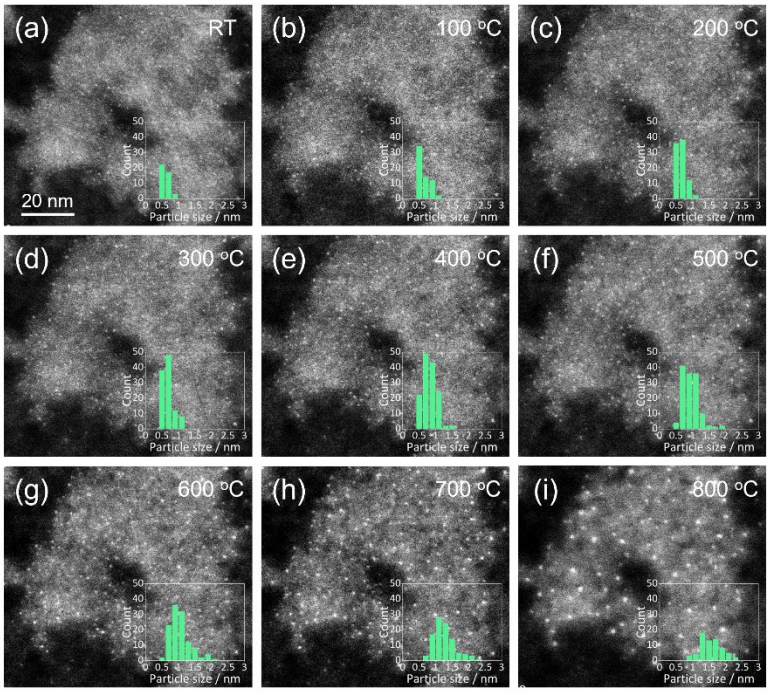

Figure S6. Investigation on the effect of electron beam irradiation toward the in situ experiment. (a-i) Stepwise evolution of Pt NPs on MXene flakes at an unexposed area. The inset in each frame of (a-i) is the corresponding size distribution for Pt NPs. The scale bar in (a) also applies to (b-i).

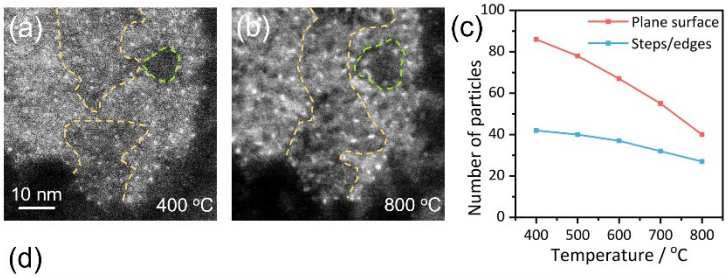

(d)

Region	Particle density / 100 nm^{-2} (400 °C)	Sintering ratio
Plane surface	5.18	53.5%
Steps/edges	4.93	35.7%

Figure S7. Investigation on the effect of surface topography of MXene for sintering of Pt NPs. (a, b) STEM images of Pt NPs on MXene flakes at 400 °C and 800 °C, respectively. (c) Number of Pt NPs as functions of heating temperature on the planar surface and steps/edges of the MXene surface. (d) The corresponding particle density and sintering ratio. The scale bar in (a) also applies to (b).

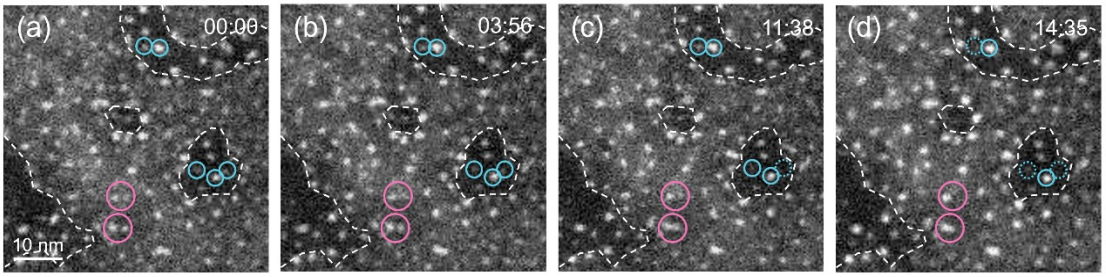

Figure S8. (a-d) A time series of STEM images showing the dynamics of PMC and OR processes for Pt NPs on the planar (pink circles) and pore (blue circles) of MXene at 800 ^{o}C. The scale bar in (a) also applies to (b-d).

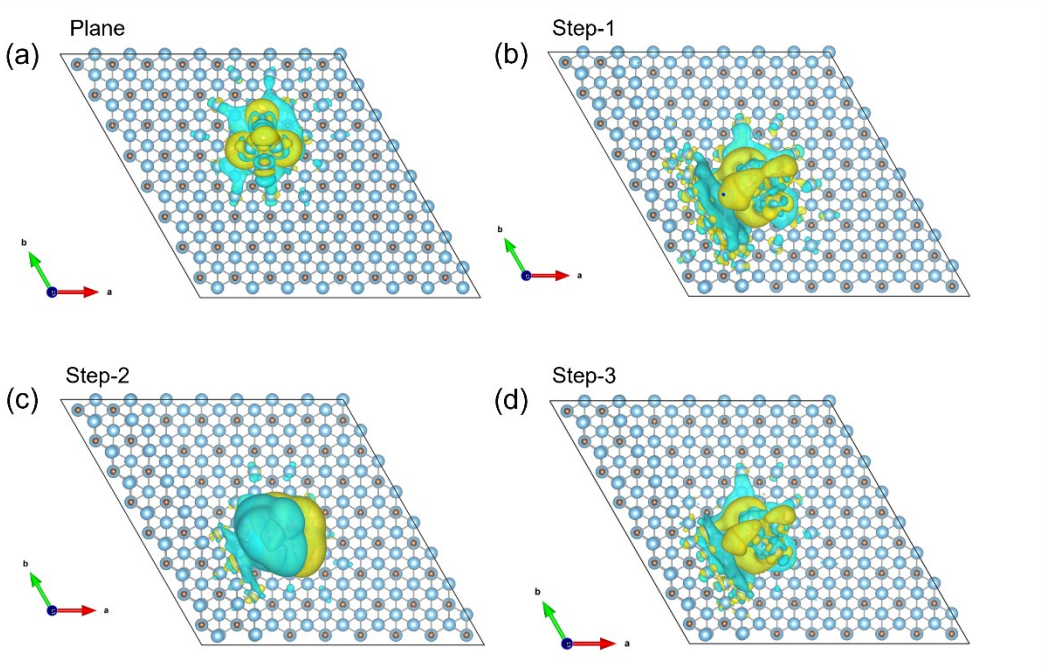

Figure S9. CCD of Pt NPs adsorbed on the (a) planar and (b-d) different positions of step regions of MXene flakes from top view (charge depletion: cyan; charge accumulation: yellow; isosurface=0.0005).

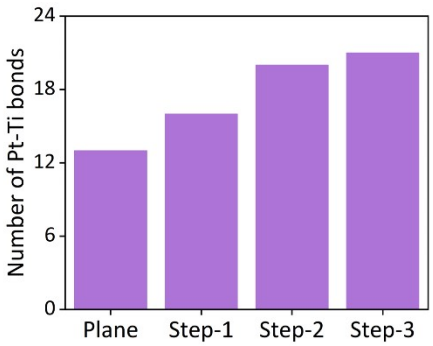

Figure S10. Number of Pt-Ti bonds with the values lower than 5.5 Å for Pt NPs adsorbed on the different positions of MXene flakes, where Plane, Step-1, Step-2 and Step-3 are the models for Pt NPs adsorbed on the planar and different step positions of MXene flakes as shown in Figure 4a-d.

3. References

1. J. P. Perdew, K. Burke and M. Ernzerhof, Generalized Gradient Approximation Made Simple, *Phys. Rev. Lett.*, 1996, **77**, 3865-3868.
2. M. Dion, H. Rydberg, E. Schröder, D. C. Langreth and B. I. Lundqvist, Van der Waals Density Functional for General Geometries, *Phys. Rev. Lett.*, 2004, **92**, 246401.